*R. Degler et al. / Geonomos, 23(2), 29-38, 2015*
*www.igc.ufmg.br/geonomos*

# P- T PATH RECONSTRUCTION IN NEOPROTEROZOIC GARNET-BEARING PARAGNEISSES FROM A METASEDIMENTARY SUCCESSION OF THE SOUTH WESTERN ARAÇUAÍ OROGEN, MINAS GERAIS, BRAZIL

Reik Degler[1], Tiago Amâncio Novo[1], Bernhard Schulz[2], Gláucia Nascimento Queiroga[3]

1 – Centro de Pesquisas Professor Manoel Teixeira da Costa, Instituto de Geociências, Universidade Federal de Minas Gerais – UFMG, Campus Pampulha, 31270-901 Belo Horizonte, MG. E-mail: reikdegler@gmailcom
2 - Institute of Mineralogy TU Freiberg/Saxony, Dept. Economic Geology and Petrology, Brennhausgasse 14, D-09596 Freiberg/Saxony, Germany
3 – Departamento de Geologia, Universidade Federal de Ouro Preto - UFOP, Campus Morro de Cruzeiro, Ouro Preto, MG

*Recebido em 10 de novembro de 2015; aceito em 30 de dezembro de 2015*

**Abstract:** This paper focuses on pressure- and temperature path analyses in paragneisses from a metasedimentary succession (MSS) in the south western Araçuaí orogen. The sampling area is limited by the Abre Campo shear zone (West) and the Rio Doce Magmatic Arc (East). This region is rich in ortho-derived metamorphic basement rocks (Mantiqueira and the Juiz de Fora complexes) and para-derived metamorphic rocks, including paragneisses interlaid by quartzites, which form the MSS. The sampled rocks are mainly compost of quartz, plagioclase, garnet, K-Feldspar, orthopyroxene and sillimanite. Measurement spot profiles through garnet porphyroblasts show a certain zonation characterised by decrease in pyrope and the increase in almandine from the core to the rim. This implies retrograde growth. Metamorphic conditions are of high amphibolite- to granulite facies with maximum pressure of ca. 6 kbar and maximum temperature of ca. 700°C. The data suggest that the cores of the garnet porphyroblasts of MSS started to grow during the final deformation stage of the Araçuaí orogen (south western part); the event of decompression is captured in the rims of the porphyroblasts and related to the gravitational collapse in the Cambrian.

**Keywords:** P-T path, metasedimentary succession, geothermobarometry, Araçuaí orogen

**Resumo:** RECONSTRUÇÃO DE TRAJETÓRIAS P-T EM PARAGNAISSES GRANADÍFEROS NEOPROTEROZÓICOS DA UMA SUCESSÃO METASSEDIMENTAR NO SUDOESTE DO ORÓGENO ARAÇUAÍ, MINAS GERAIS, BRASIL. Este estudo foca analises de caminhos de pressão e temperatura em paragnaisses de sucessão metassedimentar (SMS) da região sudoeste do Orógeno Araçuaí. A área de amostragem é limitada pela zona de cisalhamento de Abre Campo a oeste e pelo Arco Magmático Rio Doce a leste. A região é rica em rochas metamórficas de alto grau ortoderivadas (complexos Mantiqueira e Juiz de Fora do embasamento) e paraderivadas; incluindo paragnaisses intercalados a quartzitos, que formam o SMS. As rochas amostradas são compostas por quartzo, plagioclásio, granada, feldspato potássio, ortopiroxênio e sillimanita. Perfis de pontos de análise em porfiroblastos de granada mostram certo zoneamento caracterizado pela redução de piropo e por aumento de almadina do núcleo para borda; isto implica em crescimento de cristal sob condições de metamorfismo retrógrado. Condições metamórficas são de fácies anfibolito alto a granulito com um máximo de pressão de *ca*. 6 kbar e com temperatura máxima de *ca*. 700°C. Os dados sugerem que porfiroblastos de granada da SMS têm nucleação e início de crescimento durante o final da etapa deformacional principal compressiva do Orógeno Araçuaí (região sudoeste do orógeno); o evento de descompressão captado em bordas dos porfiroblastos foi relacionando ao colapso gravitacional no Cambriano.

**Palavras-chave:** Trajetórias P-T, sucessão metassedimentar, geotermobarometria, Orógeno Araçuaí

## 1. INTRODUCTION

The studied area in the south western Araçuaí orogen, at the eastern margin of the São Francisco craton is characterised by the occurrence of Paleoproterozoic basement units (the Juiz de Fora- and the Mantiqueira Complex) and a Neoproterozoic cover, the metasediments analysed in this study (Pedrosa-Soares et al. 2011 and Noce et al. 2007). The rocks of this region went through several metamorphic events and are marked by northeast to southwest trending huge deformation structures, such as the Abre Campo shear zone (Fig. 1). The geological units are clearly defined and discussed by many authors, such as Queiroga et al. 2011 and Gradim et al. 2011. Furthermore, rocks out of the metasedimentary succession (MSS) were subjected in Belém et al. 2011 and analysed by U/Pb detrital zircon dating. A missing parameter for the mentioned MSS rock samples is the reconstruction of pressure (P) and temperature (T) conditions as a key challenge to understand regional geology settings and the tectonic evolution of the south western Araçuaí orogen. Pointing out metamorphic conditions, such as P and T can be a useful tool and help to interpret present day rock assemblages. In order to constrain the conditions of crystallisation, geothermobarometry based on cation exchange and net transfer reactions has been applied to the garnet bearing metasedimentary rocks from the south western Araçuaí orogen.

## 2. REGIONAL GEOLOGY

The geological map in Figure 1 shows the contact between the Araçuaí orogen and the São Francisco Craton. The contact of the two domains is marked by a suture zone, the Abre Campo shear zone (ACSZ). The Paleoproterozoic basement is represented by amphibolite-biotite-orthogneisses of the Mantiqueira complex, which occurs west of the ACSZ and enderbitic gneisses of the Juiz de Fora complex, which crops out east of this structure (Fig. 1). The

**doi: 10.18285/geonomos.v23i2.709**

rocks of the (MSS) occur intercalated in the gneisses of the Juiz de Fora Complex.

We have opted the use of the generic term MSS by the lack of definition regarding the stratigraphic nomenclature for metasedimentary rocks in the region. Some authors choose the term Andrelândia Group or megasequence, other opt Rio Doce Group. The Andrelândia Group (Ebert, 1956) occurs in distinct areas of Ribeira and Araçuaí orogens, south and southeast of São Francisco Craton and in southern Brasilia Belt nappe system (Heilbron et al. 2004). In the studied area of the present paper the term Andrelândia Group was used by Romano & Noce 2002, Tupinambá et al. 2003, Heilbron et al. 2003, Noce et al. 2003, 2006, 2012, Horn et al. 2006, Novo et al. 2012, Gradim et al. 2012 and Queiroga et al. 2012. The Rio Doce Group (Barbosa et al. 1964) occurs exclusively in the Araçuaí orogen, north of the presented area. An overview on this unit can be found in Vieira (2007). In the focused region Féboli & Paes, 2000; Oliveira, 2000; Tuller, 2000; Vieira, 1993; Angeli et al. 1988; Carvalho & Pereira, 2000 and Pereira & Zucchetti, 2000 adopted Rio Doce Group terminology. As the purpose of this paper is independent of stratigraphic nomenclature, the term MSS will be used instead of Andrelândia or Rio Doce Group, to represent metasedimentary rocks of the region.

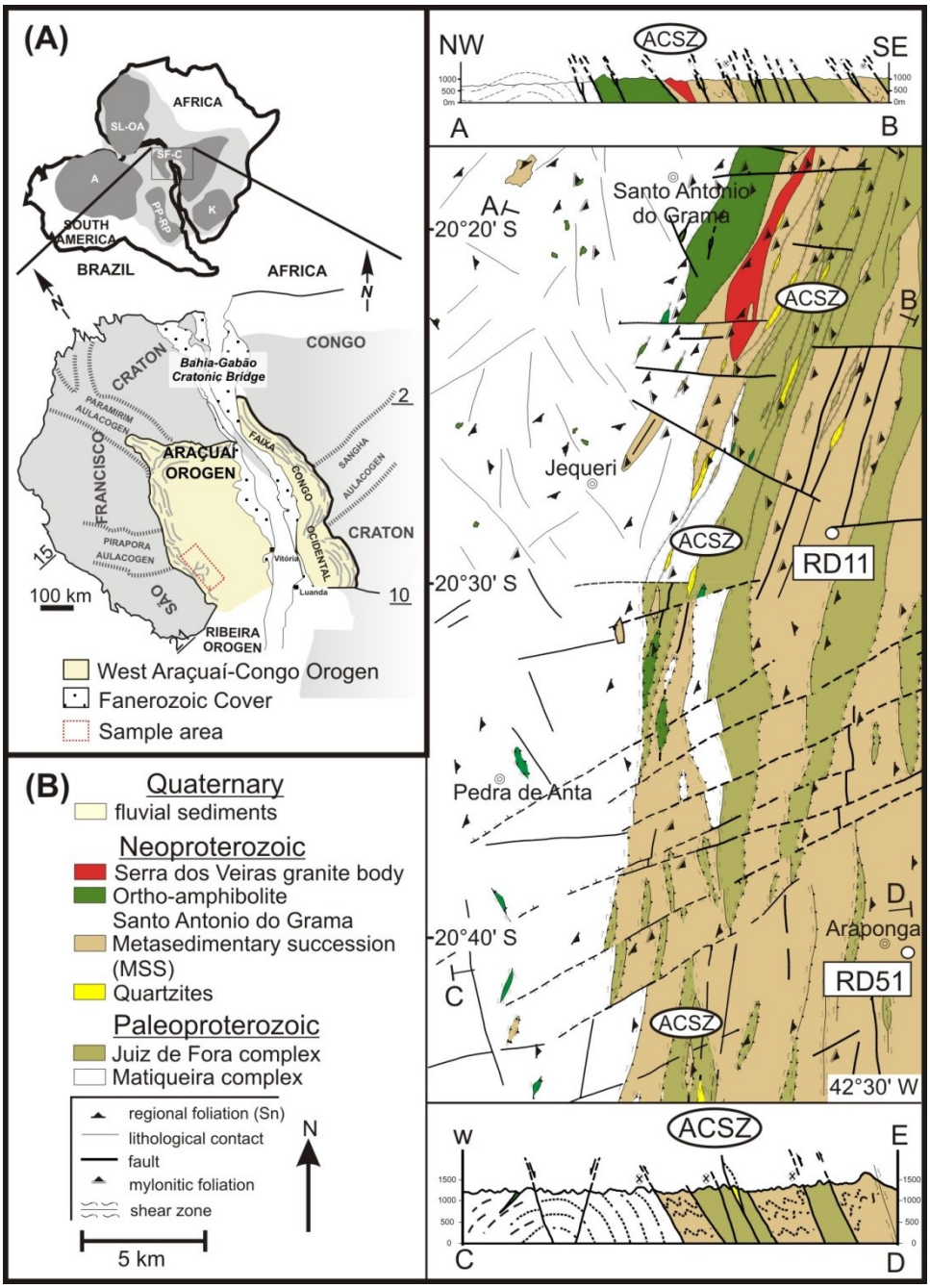


***Figure 1. (A)*** *Geotectonic setting of the Araçuaí orogeny and the São Francisco craton, with location of the study area.* ***(B)*** *Geological map of the studied area, based on Queiroga et al., 2011 and Gradim et al., 2011. ACSZ = Abre Campo shear zone.*

The most common rock of the MSS is a garnet bearing banded metasedimentary rock, which could have been generated from different sources. They show a banding from centimetre to decimetre thickness and a certain migmatization. The banding reflects the interchange of mafic, dark paleosomatic layers and leucosomatic, light ones. The general mineralogy of the paragneisses from MSS is: quartz, plagioclase, biotite, garnet, sillimanite, K-Feldspar and orthopyroxene (see Table A). The rocks often show a foliation parallel to the banding, defined by huge garnet crystals (up to 1 cm), which occur as porphyroblasts and are orientated along the foliation (compare Fig. 2b and 2c, Fig. 3). Accessory minerals are apatite, titanite, monazite and zircon. Based on geochemistry data, Belém at al. (2011) suggests that these rocks were deposited in a fore-arc basin, with mixing of sediments from a magmatic arc and from the basement. Tectonically the rocks of MSS were influenced by three phases of deformation ($D_1$, $D_2$, $D_3$). $D_3$, the most recent one, is considered to be a continuation of $D_1$ and $D_2$ and resulted in NNE-SSW trending shear zones, for example the Abre Campo shear zone (Alkmim et al. 2006).

## 3. METHODS AND SAMPLES

Two samples of a garnet bearing banded metasedimentary rock from the MSS (RD11 and RD51) were selected for geothermobarometrical analyses (Fig. 2, Table 1). Thin sections were investigated under a scanning electron microscope (SEM) Quanta 650 FEG produced by FEI Company. The instrument is equipped with two parallel Bruker X-Flash detectors for energy dispersive element analysis (EDS). The aim is to define a backscattered electron images (BSE) shade of grey value under a particular set of measurement conditions. The used Mineral Liberation Analyser (MLA) measurement mode in the present study was mapping of garnet and biotite in thin sections, called Garnet X-ray Mapping (GXMAP). This technique generates a particle mineral map (see Fig. 3) by classification of points into mineral identity. This method finds growth zones and resolves complex intergrowth. The used magnification was 100x and the distance from sample to detector is 10.9 mm.

Further, the thin sections were detected by an electron microprobe analyser with added capability of chemical analysis. The electron microprobe used in this study was JXA 8900RL, of the JEOL Company, at the Institute of Werkstoffwissenschaften in Freiberg/Saxony. The calibration of the electron beam was set as following: 20 kV/150nA with common matrix ZAF corrections.


***Figure 2.*** *Field aspects of sample RD11* ***(A)****; detailed view of the rock, showing garnet crystals up to 1 cm* ***(B)****; Field aspects of sample RD51* ***(C)****; detailed view of the rock, composed by quartz, biotite, plagioclase and garnet* ***(D)****.*

***Table 1.*** *Location and mineralogy of the samples from MSS analysed to geothermobarometry.*

| Sample | Coordinates UTM | Mineralogy |
|---|---|---|
| RD11 | 0755935/7734053 | Qtz+Pl+Bt+Grt±Kfs± Sil |
| RD51 | 0753654/7710340 | Qtz+Pl+Bt+Grt±Kfs± Sil |

## 4. GEOTHERMOBAROMETRY, P- T PATH

For geothermobarometry analyses, we attempted to identify garnet crystals as large and less perforated as possible, with complete zonation profile and inclusions (Fig. 4). High mode of biotite and plagioclase within or next to garnet crystals were also criteria necessary to take into account. Large garnet porphyroblasts with 5 mm in diameter bear numerous inclusions by quartz, biotite and opaque minerals (Fig. 4, A-E). The inclusions are not aligned with preferred orientation and define no trace of an internal relic foliation. The garnets are mostly surrounded by biotite minerals, which vary between 500 µm to 1.5 mm. Intrusions of plagioclase through the garnet porphyroblasts are rare and small. On the contrary, plagioclases in the matrix range diameters up to several millimeters (Fig. 4C, RD11-Gt3). The single spot analyses of the electron microprobe for garnet are marked by continuing numbers. Selected biotite and plagioclase is labeled with yellow letters. Zonation profiles from rim-to-core-to-rim (r-c-r) of single garnet porphyroblasts in almandine minus 60%, grossular, pyrope and spessartine are presented on the right (Fig. 4). To illustrate zonation trends of the garnets in the profiles, the data are plotted in the grossular – pyrope - spessartine ternary diagram (Fig. 5) as proposed by Schulz (1993), Schulz et al. (2001) and in a revised XCa – XMg diagram (Fig. 5, A and B) as proposed by Martignole & Nantel (1982). The mineral analyses combined for geothermobarometric calculations are as following in Table 4. The Table 4 shows the arrangement of single spot measure points for garnet (Grt), plagioclase (Pl) and biotite (Bt), which are used to calculate temperature and pressure conditions (after Holdaway 2000, Wu et al. 2004). The results are presented in the Figures (Fig. 6). To identify each analysis combinations the numbers (No.) are also given in the diagrams. The geothermobarometrical P- T paths are plotted from core (c) to rim (r). The analytic data are listed in Table 2 and 3 for each sample and can be identified by their sample names. A complete list of analytical results can be found in the Supplemental File.

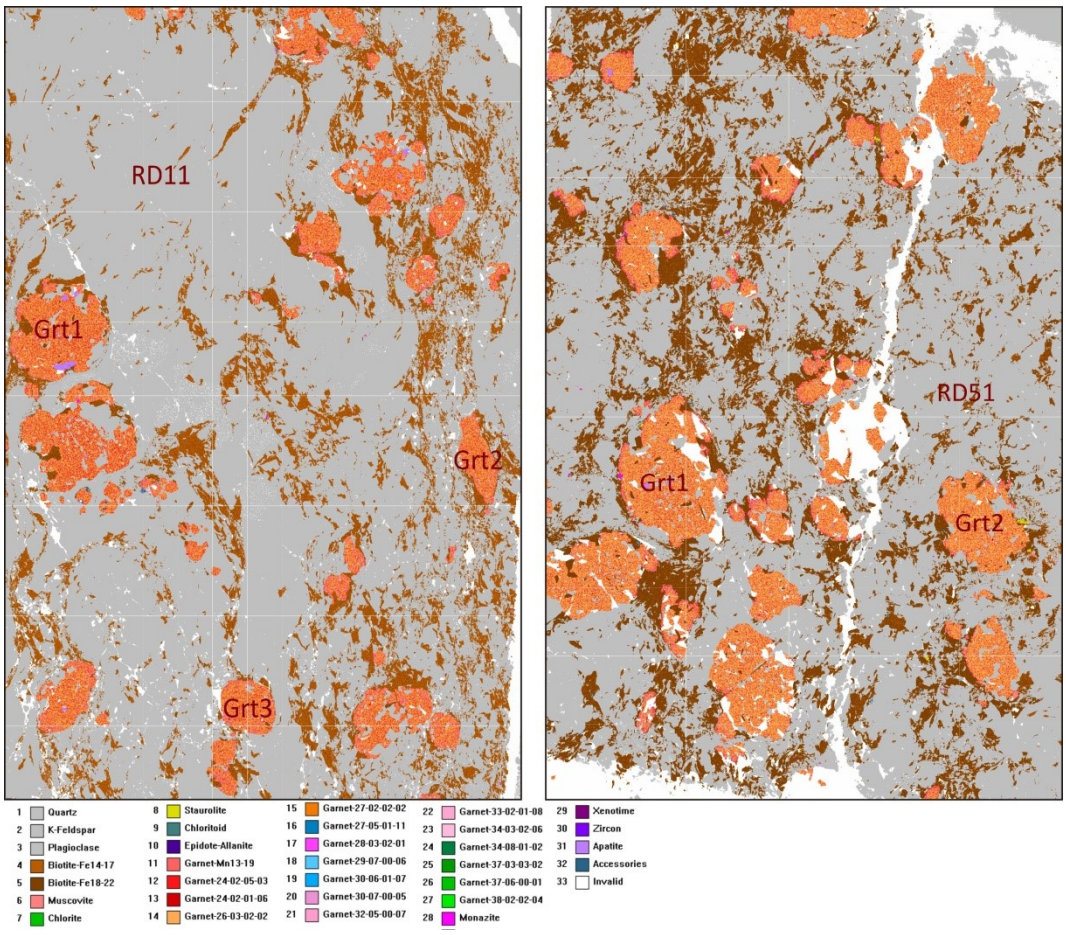


***Figure 3.*** *Grid of GXMAP analyses of the whole thin section of RD11 and RD51. The width of one thin section is 25 mm.*

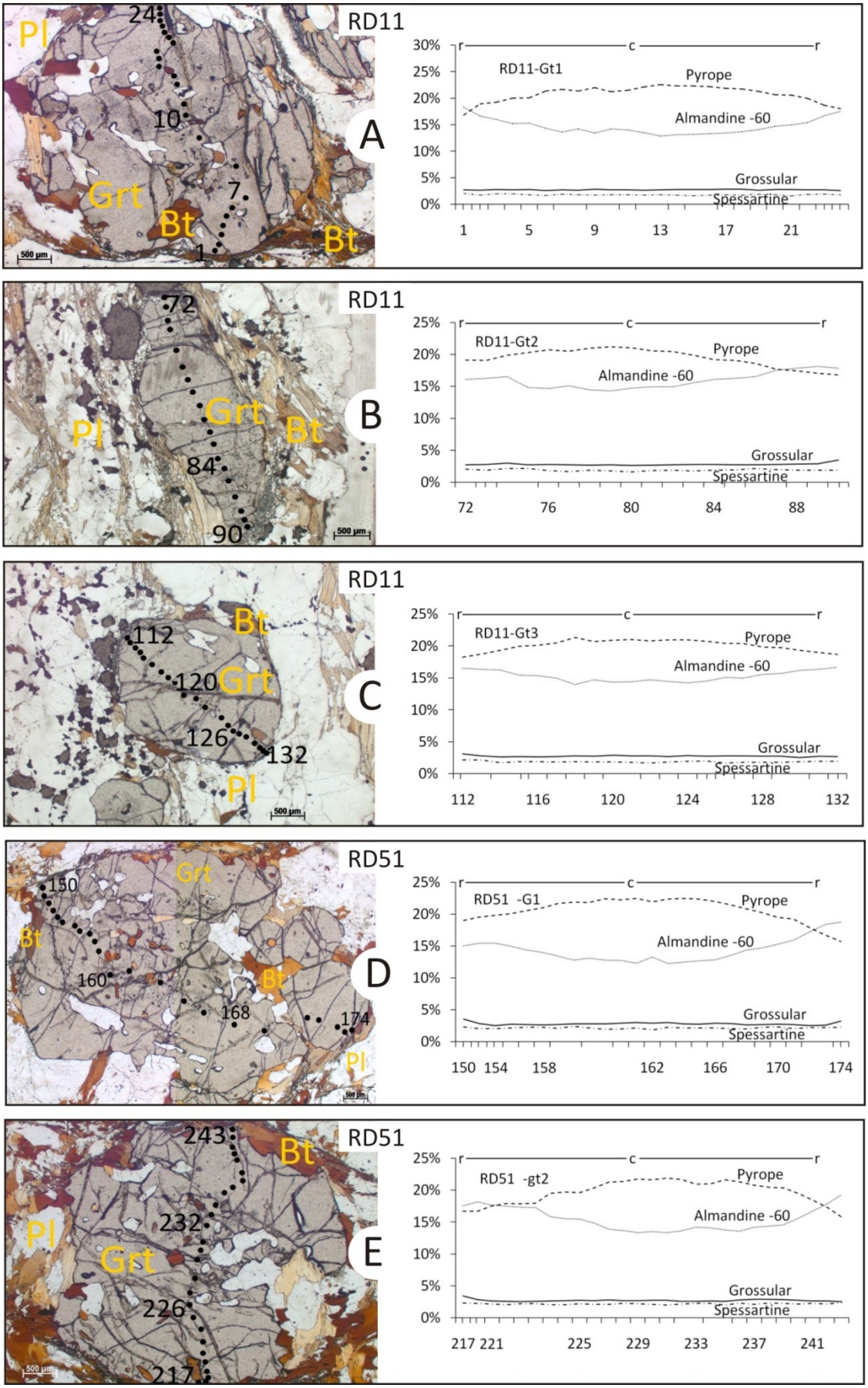


***Figura 4.*** *Microstructures around garnet porphyroblasts and garnet zonation in metasedimentary rocks RD11 (A-C) and RD51 (D-E). Garnets are surrounded by quartz, plagioclase and biotites.*

***Table 2.*** *Electron microprobe analyses (wt. %) of garnet (Grt), biotite (Bt) and plagioclase (Pl) in the metasediment of RD11, normalised to 12 O (garnet), 22 O (biotite) and 8 O (plagioclase), after Droop (1987).*

| Grt RD11 | Gt1-15 | Gt1-10 | Gt1-1 | Gt2-9 | Gt2-12 | Gt2-14 | Gt2-16 | Gt3-12 | Gt3-10 | Gt3-7 |
|---|---|---|---|---|---|---|---|---|---|---|
| **Si** | 3,01 | 3,02 | 2,99 | 3,01 | 3,02 | 3,03 | 3,02 | 3,03 | 3,02 | 3,00 |
| **Al** | 1,94 | 1,95 | 1,97 | 1,96 | 1,94 | 1,94 | 1,97 | 1,94 | 1,95 | 1,95 |
| **Fe** | 1,89 | 1,92 | 2,11 | 1,94 | 1,98 | 2,00 | 2,04 | 1,92 | 1,92 | 1,93 |
| **Mn** | 0,04 | 0,05 | 0,06 | 0,04 | 0,05 | 0,05 | 0,05 | 0,05 | 0,05 | 0,05 |
| **Mg** | 1,03 | 0,98 | 0,81 | 0,97 | 0,93 | 0,89 | 0,83 | 0,96 | 0,97 | 0,99 |
| **Ca** | 0,09 | 0,09 | 0,10 | 0,09 | 0,09 | 0,09 | 0,09 | 0,09 | 0,09 | 0,09 |
| **tot** | 8,01 | 8,00 | 8,02 | 8,01 | 8,01 | 7,99 | 8,00 | 7,99 | 8,00 | 8,02 |
| **Alm%** | 61,27 | 62,95 | 67,90 | 63,31 | 64,66 | 65,80 | 67,52 | 63,52 | 63,20 | 62,25 |
| **Prp%** | 34,23 | 32,47 | 27,01 | 32,41 | 30,75 | 29,49 | 27,62 | 31,91 | 32,15 | 32,97 |
| **Sps%** | 1,43 | 1,56 | 1,90 | 1,41 | 1,54 | 1,69 | 1,78 | 1,62 | 1,55 | 1,67 |
| **Grs%** | 3,07 | 3,02 | 3,19 | 2,87 | 3,05 | 3,02 | 3,09 | 2,95 | 3,10 | 3,10 |
| **XMg** | 0,34 | 0,33 | 0,27 | 0,32 | 0,31 | 0,30 | 0,28 | 0,32 | 0,32 | 0,33 |
| **XCa** | 0,03 | 0,03 | 0,03 | 0,03 | 0,03 | 0,03 | 0,03 | 0,03 | 0,03 | 0,03 |

| Bt RD11 | 16m-2 | 16m-1 | 12iG-2 | 12iG-1 | 14m-2 | 14m-1 |
|---|---|---|---|---|---|---|
| **Si** | 5,44 | 5,56 | 5,36 | 5,40 | 5,42 | 5,30 |
| **AlIV** | 2,56 | 2,44 | 2,64 | 2,60 | 2,58 | 2,70 |
| **AlVI** | 0,38 | 0,82 | 0,36 | 0,40 | 0,34 | 0,12 |
| **Ti** | 0,58 | 0,52 | 0,60 | 0,60 | 0,56 | 0,56 |
| **Fe** | 1,72 | 1,60 | 1,46 | 1,50 | 1,74 | 1,68 |
| **Mg** | 2,86 | 2,50 | 3,10 | 3,04 | 2,94 | 2,82 |
| **Na** | 0,02 | 0,02 | 0,10 | 0,10 | 0,02 | 0,02 |
| **K** | 1,92 | 1,64 | 1,88 | 1,84 | 1,92 | 30,4 |
| **tot** | 15,48 | 15,10 | 15,52 | 15,48 | 15,52 | 16,26 |
| **X**Mg | 0,52 | 0,46 | 0,56 | 0,55 | 0,53 | 0,54 |

| Pl RD11 | ig1-2 | 6m-8 | m-6 |
|---|---|---|---|
| **Si** | 2,73 | 2,73 | 2,71 |
| **Al** | 1,25 | 1,25 | 1,26 |
| **Ca** | 0,30 | 0,30 | 0,31 |
| **Na** | 0,73 | 0,71 | 0,74 |
| **K** | 0,01 | 0,02 | 0,02 |
| **tot** | 5,02 | 5,01 | 5,04 |
| **An** | 41,98 | 42,58 | 41,93 |

***Table 3**. Electron microprobe analyses (wt. %) of garnet (Grt), biotite (Bt) and plagioclase (Pl) in the metasediment of RD51, normalised to 12 O (garnet), 22 O (biotite) and 8 O (plagioclase), after Droop (1987).*

| Grt RD51 | G1-10 | G1-13 | G1-16 | G1-19 | G1-22 | G1-25 | gt2-15 | gt2-21 | gt2-24 | gt2-27 |
|---|---|---|---|---|---|---|---|---|---|---|
| **Si** | 3,02 | 3,01 | 3,00 | 3,03 | 3,02 | 3,01 | 3,03 | 3,02 | 3,01 | 3,00 |
| **Al** | 1,95 | 1,98 | 1,95 | 1,95 | 1,95 | 1,97 | 1,94 | 1,94 | 1,95 | 1,96 |
| **Fe** | 1,86 | 1,90 | 1,88 | 1,92 | 1,98 | 2,11 | 1,87 | 1,93 | 1,98 | 2,14 |
| **Mn** | 0,05 | 0,05 | 0,06 | 0,05 | 0,06 | 0,06 | 0,05 | 0,06 | 0,06 | 0,07 |
| **Mg** | 1,02 | 1,00 | 1,03 | 0,96 | 0,89 | 0,75 | 1,00 | 0,97 | 0,91 | 0,76 |
| **Ca** | 0,09 | 0,10 | 0,09 | 0,09 | 0,09 | 0,11 | 0,09 | 0,10 | 0,09 | 0,09 |
| **tot** | 8,00 | 8,02 | 8,01 | 8,00 | 7,99 | 8,01 | 7,99 | 8,01 | 8,01 | 8,01 |
| **Alm%** | 61,28 | 62,09 | 60,68 | 63,55 | 65,59 | 69,18 | 62,19 | 62,97 | 64,56 | 69,65 |
| **Prp%** | 33,98 | 33,12 | 34,37 | 31,75 | 29,58 | 25,06 | 33,07 | 31,95 | 30,42 | 25,27 |
| **Sps%** | 1,68 | 1,60 | 1,90 | 1,76 | 1,82 | 2,07 | 1,73 | 1,86 | 1,93 | 2,17 |
| **Grs%** | 3,07 | 3,19 | 3,04 | 2,95 | 3,02 | 3,69 | 3,01 | 3,22 | 3,10 | 2,92 |
| **XMg** | 0,34 | 0,33 | 0,34 | 0,32 | 0,30 | 0,25 | 0,33 | 0,32 | 0,30 | 0,25 |
| **XCa** | 0,03 | 0,03 | 0,03 | 0,03 | 0,03 | 0,04 | 0,03 | 0,03 | 0,03 | 0,03 |

| Bt RD51 | B10m2 | B10m1 | B3ig2 | B3ig1 |
|---|---|---|---|---|
| **Si** | 5,46 | 5,46 | 5,44 | 5,48 |
| **AlIV** | 2,54 | 2,54 | 2,56 | 2,52 |
| **AlVI** | 0,38 | 0,32 | 0,36 | 0,42 |
| **Ti** | 0,54 | 0,56 | 0,60 | 0,54 |
| **Fe** | 1,64 | 1,70 | 1,52 | 1,54 |
| **Mg** | 30,2 | 2,98 | 3,06 | 3,06 |
| **Na** | 0,02 | 0,04 | 0,02 | 0,02 |
| **K** | 1,90 | 1,92 | 1,90 | 1,86 |
| **tot** | 15,50 | 15,52 | 15,46 | 15,44 |
| **X**Mg | 0,54 | 0,54 | 0,55 | 0,55 |

| Pl RD51 | P5m10 |
|---|---|
| **Si** | 2,72 |
| **Al** | 1,25 |
| **Ca** | 0,30 |
| **Na** | 0,73 |
| **K** | 0,02 |
| **tot** | 5,02 |
| **An** | 41,66 |

***Table 4.*** *Arrangement of single microprobe analyses with data taken from Table 2 and C to calculate pressure and temperature conditions for sample* ***RD11*** *(3 paths) and* ***RD51*** *(2 paths), (after Holdaway 2000, Wu et al. 2004).*

| No. | Grt | Pl | Bt | T (°C) | P (kbar) | |
|---|---|---|---|---|---|---|
| 1 | RD11-Gt1-15 | RD11-Plig1-2 | RD11-Bt16m-2 | 715 | 6,0 | c |
| 2 | RD11-Gt1-10 | RD11-Plig1-2 | RD11-Bt16m-2 | 701 | 5,7 | |
| 3 | RD11-Gt1-1 | RD11-Plig1-2 | RD11-Bt16m-1 | 648 | 5,3 | r |
| 4 | RD11-Gt2-9 | RD11-P16m-8 | RD11-BT12iG-2 | 648 | 4,6 | c |
| 5 | RD11-Gt2-12 | RD11-P16m-8 | RD11-BT12iG-2 | 637 | 4,5 | |
| 6 | RD11-Gt2-14 | RD11-P16m-8 | RD11-BT12iG-1 | 635 | 4,4 | |
| 7 | RD11-Gt2-16 | RD11-P16m-8 | RD11-BT12iG-1 | 620 | 4,0 | r |
| 8 | RD11-Gt3-7 | RD11-P1m6 | RD11-Bt14m-2 | 709 | 5,8 | c |
| 9 | RD11-Gt3-10 | RD11-P1m6 | RD11-Bt14m-2 | 698 | 5,5 | |
| 10 | RD11-Gt3-12 | RD11-P1m6 | RD11-Bt14m-1 | 697 | 5,3 | r |

| No. | Grt | Pl | Bt | T (°C) | P (kbar) | |
|---|---|---|---|---|---|---|
| 1 | RD51a-G1-10 | RD51a-P5m10 | RD51a-B10m2 | 700 | 5,8 | c |
| 2 | RD51a-G1-13 | RD51a-P5m10 | RD51a-B10m2 | 695 | 5,8 | |
| 3 | RD51a-G1-16 | RD51a-P5m10 | RD51a-B10m2 | 700 | 5,7 | |
| 4 | RD51a-G1-19 | RD51a-P5m10 | RD51a-B10m1 | 690 | 5,1 | |
| 5 | RD51a-G1-22 | RD51a-P5m10 | RD51a-B10m1 | 669 | 4,7 | |
| 6 | RD51a-G1-25 | RD51a-P5m10 | RD51a-B10m1 | 625 | 3,6 | r |
| 7 | RD51a-gt2-15 | RD51a-P5m10 | RD51a-B3ig2 | 671 | 5,3 | c |
| 8 | RD51a-gt2-21 | RD51a-P5m10 | RD51a-B3ig2 | 660 | 5,2 | |
| 9 | RD51a-gt2-24 | RD51a-P5m10 | RD51a-B3ig1 | 647 | 4,8 | |
| 10 | RD51a-gt2-27 | RD51a-P5m10 | RD51a-B3ig1 | 603 | 3,3 | r |

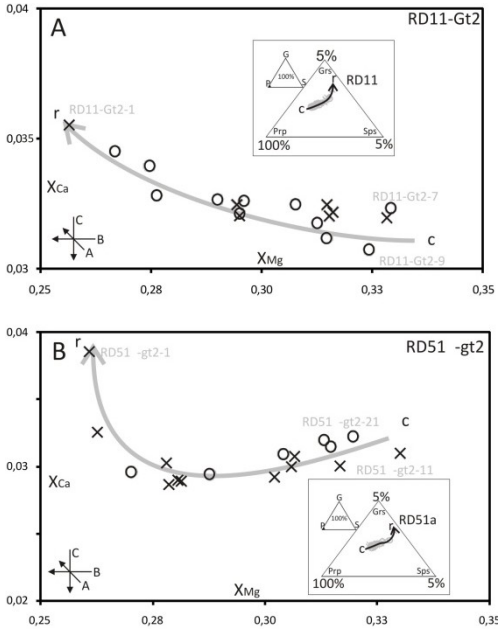


***Figura 5. (A, B):*** *Overall evolution of garnet compositions in grossular (Grs), pyrope (Prp), and spessartine (Sps) ternary components from the metasedimentary rocks of samples RD11 and RD51. Arrows characterize the core-to-rim (c, r) evolution, assembled from several analysed porphyroblasts in a sample. Analyses used for thermobarometry are presented in Table 2 and 3. (A, B): Garnet-core-to-rim (c, r) zonation trends in XMg vs. XCa coordinates. Semiquantitative P- T evolutions trends of isobaric heating expressed by XCa-XMg (after Martignol & Nantel 1982).*

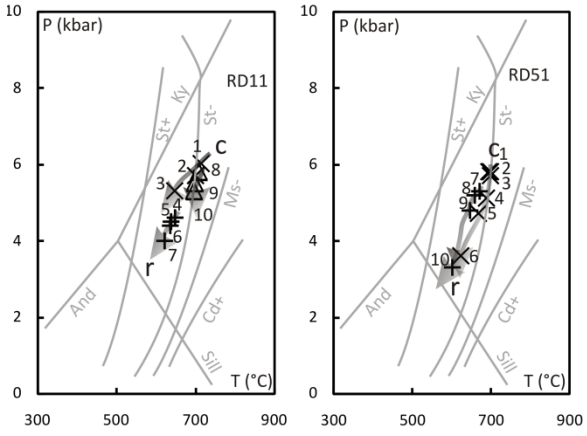


***Figure 6:*** *P- T estimates and P- T paths of sample* ***RD11*** *and* ***RD51****. Numbers are characteristic garnet analyses in Tables D. Large symbols represent P- T results from the garnet-biotite thermometer and the GASP barometer (see text), enclosing an error of ± 50 °C and ± 1 kbar. STability fields for kyanite (Ky), andalusite (And), sillimanite (Sil) and staurolite-in (St+); staurolite-out (St-), cordierite-in (Cd+) and muscovite-out (Ms-) are marked for general orientation by univariant reaction lines (after Spear 1993). Distinct mineral chemical zonation trends observed in garnet porphyroblasts (Figure 4 and Figure 5 A, B) correspond to segmental trends during garnet crystallisation in limited assemblage with biotite and plagioclase and quartz.*

## 5. CONCLUSION

*Garnet zoning:* The zoning characteristics of the metasedimentary garnets of RD11 and RD51 are shown in Figure 4 A - E. The decrease in pyrope and the increase in almandine from the core to the rim of the garnet imply retrograde growth.

*Plagioclase zoning:* The retrograde plagioclases in matrix or within garnets of RD11 and RD51 have similar compositions. They are unzoned and characterised by almost no variation of Ca content. This suggests the same evolutional stages for the plagioclase as for the garnet and confirms a retrograde reaction.

*Biotite zoning:* There was no noticeable variation of XMg or Ti content in the biotite grains. Also biotite within garnet or in matrix shows no differences. To guaranty comparable data results sometimes the same biotite analyses point was used for several garnet spot points.

The detailed analyses of garnet, plagioclase and biotite were necessary to require best fitting conditions for P- T path recapitulation.

*P-T conditions:* The retrograde evolution of the metasedmiments is dominated by decompression to P < 6 kbar. The abundant retrograde reactions provide an excellent possibility for the application of used geothermobarometers. The reaction of decompression and decrease of temperature from core to rim can be divided as followed into different stages. After burial and prograde evolution with peak-metamorphic conditions the material rises and pressure and temperature conditions change, they decrease (Fig. 6). Between temperatures of 630 – 700°C garnet start to regrow and is characterised by almost unzoned appearance (Brandt et al. 2003). This weak zonation explains also the small range of calculated temperature and pressure (compare Fig. 6 and Table 4). Furthermore, conditions of 650°C and 5 kbar indicate that garnet and biotite regrowth response to near-isobaric cooling (Brandt et al. 2003).

The geothermobarometric data confirm with metamorphic conditions, so far described for this region (Gradim et al. 2011). With $T_{max}$ of ca. 700°C and $P_{max}$ of ca. 6 kbar the rocks of the MSS in the south western Araçuaí orogen can be described as in transitions between granulite and amphibolite metamorphic facies. The decompression-cooling retrograde reactions of RD11 and RD51 indicate and uplift from mid-crustal level (ca. 18 km), which probably took place along regional shear zones during the evolution of the Araçuaí orogen.

## 6. ACKNOWLEDGMENT

The authors acknowledge financial support by the DAAD. Suggestions and reviews provided by Matheus Kuchenbecker greatly improved the original manuscript.

## 7. REFERENCES

Alkmim F.F., Marshak S., Pedrosa-Soares A.C., Peres G.G., Cruz S.C.P., Whittington A. 2006. Kinematic evolution of the Araçuaí-West Congo orogen in Brazil and Africa: Nutcracker tectonics during the Neoproterozoic assembly of Gondwana. *Precambrian Res.*, 149: 43-63.

Angeli N. 1988. Pesquisa dos jazimentos de níquel e geologia da Folha Ipanema, MG. Tese de Doutorado, Instituto de Geociências, Universidade de São Paulo, 290p.

Barbosa A.L. de M., Grossi Sad J.H., Torres N., Melo M.T.V. 1964. Geologia das quadrículas de Barra do Cuieté e Conselheiro Pena, Minas Gerais. Belo Horizonte, DNPM/GEOSOL, 285 p.

Brandt, S., Klemd, R., And Okrusch, M. (2003). Ultrahigh-Temperature Metamorphism and Multistage Evolution of Garnet-Orthopyroxene Granulites from the Proterozoic Epupa Complex, NW Namibia. Journal of Petrology, 44: 1121-1144.

Carvalho J.B., Pereira L.M.M. 2000. Projeto Leste: Petrografia, relatório integrado. Etapa II. Belo Horizonte: SEME/CPRM/CODEMIG, CD-ROM.

Droop G.T.R. (1987). A general equation for estimating Fe3+ concentrations in ferromagnesian silicates and oxides from microprobe analyses, using stoichiometric criteria. Min. Mag. 51, 431-435.

Ebert H. 1956. A tectônica do sul do Estado de Minas Gerais e regiões adjacentes. In: Relatório Anual do Diretor, ano 1955, DGM, Rio de Janeiro : p. 97-107 e p. 136-137.

Féboli & Paes 2000. Projeto Leste-MG. Folha Itanhomi (SE.24-Y-C-I), Belo Horizonte, SEME/COMIG/CPRM, escala 1:100.000.

Gradim D.T., Noce, C.M., Novo T., Queiroga G.N., Pedrosa-Soares A.C., Suleimam M.A., Martins M. 2012. Mapa geológico da Folha Viçosa (SF.23-X-B-V), Belo Horizonte, CPRM/UFMG, escala 1:100.000.

Gradim D.T., Queiroga G.N., Novo T., Noce C.M., Pedrosa-Soares A.C., Romano A.W., Martins M., Alkmim F.F., Bastos C.F., Suleimam M.A. 2011. Geologia da região de Jequeri-Viçosa (MG), Orógeno Araçuaí Meridional. Geonomos, 19(2):107-201.

Heilbron M.L., Pedrosa-Soares A.C., Campos Neto M.C., Silva L.C., Trouw R. & Janasi V.A. 2004. Província Mantiqueira. In: V.M. Mantesso-Neto, A. Bartorelli, C.D.R. Carneiro & Brito-Neves, B.B. (orgs.). Geologia do Continente Sul-Americano.São Paulo, Editora Beca, p. 203-234.

Heilbron M., Tupinambá M., Duarte B., Eirado L., Nogueira J., Prado J., Sucena M. 2003. Geologia da Folha Leopoldina (SF.23-X-D-V). Belo Horizonte, COMIG/UFMG/UFRJ/UERJ - Projeto Sul de Minas, escala 1:100.000.

Holdaway, M.J. (2001). Recalibration of the GASP geobarometer in light of recent garnet and plagioclase activity models and versions of the garnet-biotite geothermometer. – American Mineral., Washington D. C. (Mineral. Soc. America) 86: 1117–1129.

Horn A., Faria B., Gardini G., Vasconcellos L., Oliveira M. 2006. Geologia da Folha Espera Feliz. Rio de Janeiro, CPRM-Serviço Geológico do Brasil, UFMG-Programa Geologia do Brasil, escala 1:100.000.

Martignole, J. & Nantel, S. (1982). Geothermobarometry of cordierite-bearing metapelites near the Morin anorthosite complex, Grenville province, Quebec. Canadian Mineralogist, Montreal (NRC Research Pr.). 20: 307–318.

Noce C.M., Novo T., Figueiredo C., Pedrosa-Soares A. C. 2012. Mapa geológico da Folha Carangola (SF.23-X-B-VI). Belo Horizonte, CPRM/UFMG, escala 1:100.000.

Noce C.M., Pedrosa-Soares A.C., Silva L.C., Armstrong R. & Piuzana D. 2007. Evolution of polyciclic basement complexes in the Araçuaí orogen, based on U–Pb SHRIMP data: Implications for Brazil–Africa links in Paleoproterozoic time. Precambrian Research, 159: 60-78.

Noce, C.M., Novo T., Figueiredo, C., Pedrosa-Soares, A. C. 2006. Mapa geológico da Folha Manhuaçu (SF.23-X-B-III). Rio de Janeiro, CPRM/UFMG - Programa Geologia do Brasil, escala 1:100.000.

Noce C.M., Romano A.W., Pinheiro C.M., Mol V.S., Pedrosa-Soares A.C. 2003. Geologia das Folhas Ubá e Muriaé. In: A.C. Pedrosa-Soares, C.M. Noce, R. Trouw, M. Heilbron (coords.). Projeto Sul de Minas – Etapa I: Geologia e Recursos Minerais do Sudeste Mineiro. COMIG/UFMG/UFRJ/UERJ, Belo Horizonte, cap.12, p.623-659.

Novo T., Noce, C.M., Batista G., Quéméneur J., Martins, B., Santos, S., Carneiro G., Horn, A. 2012. Mapa geológico da Folha Manhumirim, (SF.24-V-A-I). Belo Horizonte, CPRM/UFMG, escala 1:100.000.

Queiroga G.N., Gradim D.T., Pedrosa-Soares A.C., Pinho R.R., Vilela F., Noce C.M., Nola T., Novo T.A., Suleimam M.A., Basto C.F. 2012. Folha Jequeri SF-23-X-B-II-4, escala 1:50.000. Contrato CPRM-UFMG-Programa Geologia do Brasil.

Schulz, B. (1993). P-T-deformation paths of Variscan metamorphism in the Austroalpine basement: controls on geothermobarometry from microstructures in progressively deformed metapelites. – Swiss Bull. Mineral. Petrol., Zürich (Staeubli). 73: 257–274.

Schulz, B., Triboulet, C., Audren, C. & Feybesse, J.-L. (2001). P-T paths from meta pelite garnet zonations, and crustal stacking in the Variscan inverted meta morphic sequence of La Sioule, French Massif Central. – Z. dt. geol. Ges., Stuttgart (Schweizerbart) 152: 1–25.

Spear, F.S. (1993). Metamorphic phase equilibria and pressure temperature-time paths. – Mineral. Soc. America, Monogr., Washington D. C. (Mineral. Soc. America). 1: 799.

Pedrosa-Soares A.C., Noce C.M; Alkmim F.F., Silva L.C., Babinski M., Cordani U., Castañeda C. 2007. Orógeno Araçuaí: síntese do conhecimento 30 anos após Almeida 1977. Geonomos, 15 (1): 1-16.

Pedrosa–Soares A.C., De Campos C., Noce C.M., Silva L.C., Novo T., Roncato J., Medeiros S., Castañeda C., Queiroga G., Dantas E., Dussin I., Alkmim F.F. 2011. Late Neoproterozoic–Cambrian granitic magmatism in the Araçuaí orogen (Brazil), the Eastern Brazilian Pegmatite Province and related mineral resources. Geological Society, London, Special Publications, 350: 25-51.

Pereira L. M. M. & Zucchetti M. 2000. Projeto Leste: Petrografia, relatório integrado. Etapa II. Belo Horizonte: SEME/CPRM/CODEMIG, CD-ROM.

Romano, A.W. & Noce, C.M. 2003. Geologia da Folha Muriaé (SF.23-X-D-III). Belo Horizonte, COMIG/UFMG/UFRJ/UERJ - Projeto Sul de Minas, escala 1:100.000.

Tuller, M. 2000. Projeto Leste-MG. Folha Ipanema (SE.24-Y-C-IV), Belo Horizonte, SEME/COMIG/CPRM, escala 1:100.000.

Tupinambá, M., Almeida, C., Eirado, E., Duarte, B., Heilbron, M. 2003. Geologia da Folha Pirapetinga (SF.23-X-D-VI). Belo Horizonte, COMIG/UFMG/UFRJ/UERJ - Projeto Sul de Minas, escala 1:100.000.

Vieira, V.S. 2007. Significado do Grupo Rio Doce no Contexto do Orógeno Araçuaí. Tese de Doutorado, Instituto de Geociências, Universidade Federal de Minas Gerais, 117p.

Wu, C.M., Zhang, J. And Ren, L.D (2004). The GBPQ Barometer: Empirical garnet –biotite–plagioclase–quartz (GBPQ) geobarometry in medium– to high–grade metapelites. Journal of Petrology, 45: 1907-1921.